10-2-2002

Multiscale nature of hysteretic phenomena: Application to CoPt-type magnets

Kirill D. Belashchenko
University of Nebraska-Lincoln, belashchenko@unl.edu

Vladimir P. Antropov
Ames Laboratory, US Department of Energy, antropov@ameslab.gov

Multiscale nature of hysteretic phenomena: Application to CoPt-type magnets

K. D. Belashchenko and V. P. Antropov
Ames Laboratory, Ames, Iowa 50011
(Received 14 May 2002; published 4 October 2002)

We suggest a workable approach for the description of multiscale magnetization reversal phenomena in nanoscale magnets and apply it to CoPt-type alloys. We show that their hysteretic properties are governed by two effects originating at different length scales: a peculiar splitting of domain walls at twin boundaries and their strong pinning at antiphase boundaries. We emphasize that such multiscale nature of hysteretic phenomena is a generic feature of nanoscale magnetic materials.

DOI: 10.1103/PhysRevB.66.144402 PACS number(s): 75.60.Ch, 73.20.−r, 75.50.Ww, 75.60.Jk

I. INTRODUCTION

The problem of magnetization reversal is a central and longstanding problem in the theory of magnetism. The main complications in its treatment stem from the fact that effects due to magnetostatic and elastic forces manifest themselves in the whole nanoscale range while local interactions must still be treated on the atomistic scale. As the length scale increases, new physical effects arise, but coarse-graining over the lower-scale degrees of freedom is not easily accomplished. Specifically, magnetization reversal is realized by the motion of domain walls, the two-dimensional surfaces where magnetization changes its direction. Domain walls may easily move unless they are pinned by defects, which implies that magnetization reversal properties are not intrinsic and depend strongly on the microstructure. Experimentally, this results in huge variations of the coercive force H_c and other properties depending on material processing. It is crucial to address the domain wall structure and its interaction with microstructure on different length scales ranging from interatomic to submicron.

In modern micromagnetic methods[1] complex microstructures of hard magnets are defined by fields of macroscopic material properties such as the exchange constant $A(\mathbf{r})$ and the magnetocrystalline anisotropy (MCA) constant $K(\mathbf{r})$. Such calculations were mainly focused on the role of grain boundaries; since they are extremely hard to describe microscopically, their properties are postulated in an *ad hoc* manner, making reliable predictions problematic. On the other hand, typical microstructures of hard magnets with $L1_0$ crystal structure including CoPt, FePt, and FePd are dominated by other defects,[2–7] antiphase boundaries and twin boundaries, which are crystallographically coherent and easier to treat than grain boundaries. Although these materials were used and studied for many decades and the formation of their microstructure is well understood, the mechanism of magnetization reversal is still a mystery.

Microstructural evolution during $L1_0$ ordering is strongly affected by tetragonal lattice distortions.[5,6] After a relatively short ''tweed'' stage of annealing after quench, when the ordered domains achieve some characteristic size $l_0 \sim 10$ nm, they develop so-called polytwinning, i.e., the formation of regular stacks of ordered bands (''c-domains'') separated by twin boundaries.[2–6] The tetragonal axes c of the c-domains (pointing along one of the three cubic axes of the parent fcc phase) alternate regularly, making 90° angles between the adjacent domains (below we use the obvious terms ''X-domain,'' ''XY-stack,'' etc.). In addition to polytwinning, the observed and simulated microstructures always contain a high density of antiphase boundaries in the c-domains.[3–7]

Polytwinned magnets were extensively studied with analytical micromagnetic methods.[2] Due to high MCA, the domain wall width $\delta=\pi\sqrt{A/K}$ is quite small (5–10 nm), while the anisotropy field $H_a=2K/M$ (M is the saturation magnetization) significantly exceeds the typical magnetostatic field $H_m=4\pi M$ [parameter $\eta=H_m/H_a$ is close to 0.1 in CoPt and FePt and 0.38 in FePd (Ref. 2)]. Therefore, at $d\gtrsim\delta$ (d is the c-domain thickness) each c-domain may be regarded as an individual magnetic domain with intrinsic 90° domain walls at the twin boundaries.[2] It is assumed that magnetization reversal is associated with ''macrodomain walls'' crossing many c-domains. Such walls were observed experimentally,[2,4] but their internal structure and mechanisms of coercivity are unknown.[2]

The goal of the present paper is to lay the foundation of a consistent multiscale theory of magnetization reversal in CoPt-type magnets. In Sec. II we describe the microscopic mean-field method used in the simulations. Equilibrium structure of macrodomain walls in a defect-free system is addressed in Sec. III, and a peculiar splitting of macrodomain walls in external field is explained in Sec. IV. In Sec. V we discuss pinning of domain walls at antiphase boundaries and deduce the combined effect of macrodomain wall splitting and pinning on the coercivity.

II. MICROSCOPIC MEAN-FIELD METHOD

Consider a binary alloy AB with the classical Hamiltonian

$$H=H_{\mathrm{conf}}\{n_i\}+\sum_{i<j} n_i n_j[-J_{ij}\vec{\mu}_i\vec{\mu}_j+\vec{\mu}_i\hat{D}_{ij}\vec{\mu}_j]$$

$$+\sum_i n_i[\epsilon_i(\vec{\mu}_i)-\mathbf{H}_0\vec{\mu}_i], \qquad (1)$$

where H_{conf} is the configurational part of the Hamiltonian, i and j run over lattice sites, $n_i=1$ if site i is occupied by a magnetic atom A and $n_i=0$ otherwise (let B be nonmagnetic for simplicity, $\vec{\mu}_i$ is the rigid classical magnetic moment of the atom at site i, J_{ij} are the Heisenberg exchange parameters, $\mathbf{H}_0$ is the external magnetic field, $\epsilon_i(\vec{\mu}_i)$ is the MCA

energy equal to $-b_i(\vec{\mu}_i\mathbf{e}_i)^2$ for easy-axis anisotropy, and $\hat{D}_{ij}$ is the magnetic dipole-dipole interaction tensor.

The free energy in the mean-field approximation (MFA) may be related to the ''mean fields'' $\mathbf{H}_i=\mathbf{H}_0+\Sigma_j(J_{ij}-\hat{D}_{ij})c_j\mathbf{m}_j$, where $\mathbf{m}_i=\langle\vec{\mu}_i\rangle$ and $c_i=\langle n_i\rangle$ are local magnetizations and concentrations, respectively:

$$F=-E_{J,DD}-T\sum_i c_i\ln\int d\hat{\mu}_i\exp[\beta(\mathbf{H}_i\vec{\mu}_i-\epsilon_i)]. \quad (2)$$

Here $E_{J,DD}=\Sigma c_i c_j\mathbf{m}_i(-J_{ij}+\hat{D}_{ij})\mathbf{m}_j$ is the total exchange and dipole-dipole energy. Equilibrium states may be found using self-consistency relation $\mathbf{m}_i=-\partial F/\partial\mathbf{H}_i$.

If magnetization $\mathbf{M}(\mathbf{r})$ slowly varies in space and is constant in magnitude, Eq. (2) reduces to the micromagnetic free energy.[9] In this case all choices of J_{ij} and b_i in the defect-free regions are equivalent if they produce the same macroscopic properties A and K. However, variation of J_{ij} and b_i near defects like antiphase boundaries must be studied using first-principles techniques. Microscopic MFA calculations with these parameters may be used to describe domain wall interactions with a defect at the length scale of δ. At larger, microstructural length scales micromagnetic methods[1] may be used with singularities of A and K at the defects. However, in hard magnets the microscopic approach also turns out to be convenient for studies of regions containing up to $\sim 10^6$ atoms; in such calculations some model J_{ij} and b_i reproducing the actual defect properties may be used.

III. EQUILIBRIUM MACRODOMAIN WALLS

It is convenient to use the body-centered tetragonal (bct) representation of the fcc lattice (with $c/a=\sqrt{2}$ and c equal to the fcc lattice parameter). Two opposite edges of the rectangular simulation box are aligned with the (110) twin boundaries in the XY-stack; macrodomain walls are normal to them. The boundary conditions are periodic, and the dipole-dipole fields are computed using the Fourier transforms.

Equilibrium macrodomain walls of two characteristic (110) and (001) orientations are shown in Fig. 1 for the CoPt model. An infinite stack of c-domains is assumed with ideal twin boundaries in the (110) planes. Fully ordered c-domains have the same thickness $d=64a\simeq 17$ nm, which corresponds to an early stage of annealing shortly after the polytwinned stacks are formed.[4,6] The anisotropy is uniaxial with $\mathbf{e}_i$ pointing along the local direction of the tetragonal axis and $b_i=b$. Room temperature $T=0.4T_c$ is assumed averywhere (for CoPt, $T_c\simeq 720$ K). For simplicity, only $3d$-metal atoms are assumed to have magnetic moment μ. Parameters b and μ were chosen so that the MFA gives experimental room-temperature values of $K=4.9\times 10^7$ erg/cm^3 and $\eta=0.082$ for CoPt.[2] The parameters J_{ij} for nearest and next-nearest neighbors were chosen as $J_2/J_1=2/3$ and $J_3/J_1=1/6$; A is isotropic with this choice.

Macrodomain walls of both orientations shown in Fig. 1 have a peculiar feature which turns out to be the key to understanding magnetization reversal in polytwinned magnets: the domain wall segments located in adjacent c-domains are displaced in respect to each other. Such a configuration with regularly alternating displacements is beneficial for the exchange energy because the magnetization within each domain wall segment is parallel to that in the adjacent c-domains [note that the color of horizontal domain wall segments in Figs. 1(a) and 1(c) matches that of adjacent c-domains]. The magnetostatic energy for this macrodomain wall configuration is higher compared to the rectilinear one due to the presence of short magnetically charged (in micromagnetic terms[9]) segments of 90° domain walls at the twin boundaries [note the red and blue ''blobs'' in Fig. 1(d)]. The actual macrodomain wall configuration emerges as a result of competition between these interactions. However, due to small η, the dipole-dipole interaction is, in fact, unimportant at the length scale of δ.

As it is clear from Fig. 1, the magnetic charges both at the segments of a (110) macrodomain wall and at the twin boundaries alternate in sign, so that each macrodomain wall is magnetically uncharged as a whole, and its magnetic field quickly falls off at $r\gtrsim d$. Segments of (001) macrodomain walls do not carry magnetic charge.

The orientation of segments within c-domains in $(\bar{1}10)$ macrodomain wall is determined by the anisotropy of the exchange constant $\alpha=A_\perp/A_\parallel$ ($A_\perp$ and $A_\parallel$ are values of A normal and parallel to c) and by the parameter $\xi=\eta d/\delta$. At $\xi\ll 1$ the domain wall orientation is determined solely by α. At $\xi\gg 1$ the domain wall aligns parallel to the tetragonal axis, and α is irrelevant. The (110) macrodomain wall shown in Figs. 1(a) and 1(b) is in the crossover region with $\xi\sim 0.2$ and $\alpha=1$.

IV. PARTIAL MACRODOMAIN WALLS

Macrodomain walls behave remarkably in external magnetic field $\mathbf{H}_0$ because domain wall segments are held together only by magnetostatic forces. If these forces were absent ($\eta\to 0$ limit), each domain wall segment would be able to move freely until it meets another segment in an adjacent c-domain. Some of this freedom remains at small η. Consider an XY-stack with (110) twin boundaries, as above. The component H_z does not exert any force on domain wall segments, and the effect of $\mathbf{H}_0$ on macrodomain walls depends only on the orientation of its projection $\mathbf{H}_\perp$ on the xOy plane. If $\mathbf{H}_\perp$ is normal to the twin boundaries ($H_x=H_y$), then the forces acting on all domain wall segments are in the same direction, and both macrodomain walls shown in Fig. 1 move as a whole like the usual domain walls in a homogeneous crystal. However, if $\mathbf{H}_\perp$ is parallel to the twin boundaries ($H_x=-H_y$), the forces acting on X- and Y-segments differ in sign, and the total force acting on the macrodomain wall is zero.

Let us call a set of segments of a macrodomain wall in all even or odd c-domains as a *partial macrodomain wall*, e.g., X-PMDW. There are two macrodomain wall realizations differing in the sign of the relative displacement L of the two partial macrodomain walls. For one of them $\mathbf{H}_\perp$ increases $|L|$ (''splitting'') and for the other reduces it (''swapping''). If $\mathbf{H}_\perp$ is inverted, splitting turns to swapping and vice versa. Accordingly, two threshold fields may be introduced. Let us

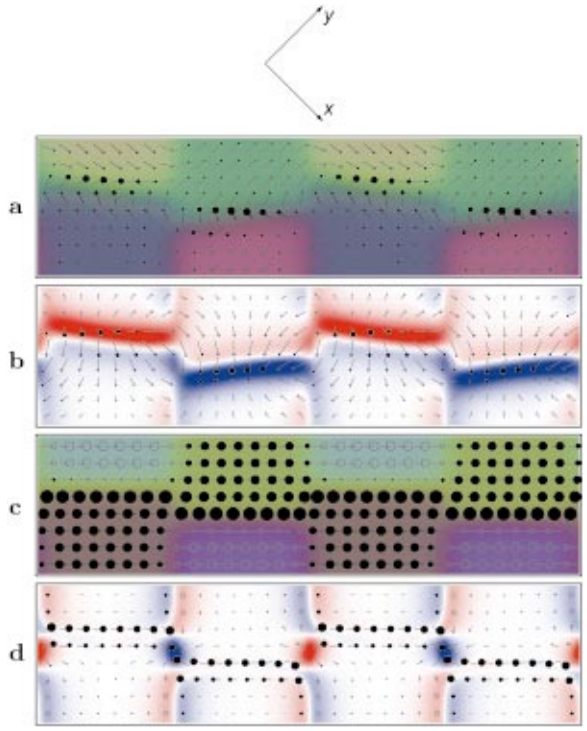

FIG. 1. (Color) Macrodomain walls in an ideal XY-stack with $d=64a_{\mathrm{bct}}$ oriented normal to (a),(b) $(1\bar{1}0)$; (c),(d) (001). (a),(c). Magnetization $\mathbf{M}(\mathbf{r})$ (arrows and color); (b),(d) dipole fields (arrows) and magnetic charge density $\rho=-\mathrm{div}\,\mathbf{M}$ (color). The axes at top refer to (a),(b); in (c),(d) they are rotated 90° around the horizontal line. Sticks with circles show vector directions for cells $i=(8n_1+4,8n_2+4,1)$ with integer n_1, n_2. The length of a stick (up to the center of the circle) is proportional to the vector projection onto the graph plane; the diameter of solid (open) circles, to the positive (negative) out-of-plane component. Small points at the end of long sticks show their direction. Color in (a),(c) (guide to the eye) is obtained by mixing red, green, and blue according to the values of three vector components. In (b),(d) the intensity of red (blue) color is proportional to the normalized density of positive (negative) magnetic charges $\rho/|\rho_{\max}|$. Twin boundaries are vertical. The simulation boxes had $128\times512\times1$ and $128\times512\times2$ bct cells for (110) and (001) macrodomain walls, respectively. Boundary conditions are periodic. Figures are 2 times wider than the simulation boxes; they are trimmed at top and bottom to conserve space.

fix, for instance, Y-PMDW and examine the effect of H_x on X-PMDW. The *threshold splitting field* H_{sp} is the minimal value of H_x required to move the X-PMDW far from the Y-PMDW. The *threshold swapping field* H_{sw} is required to ''drag'' the X-PMDW through Y-PMDW in the opposite direction, overcoming the exchange barriers at the twin boundaries. H_{sw} is of lesser importance than H_{sp} because even if $H_{\mathrm{sp}}<H_{\mathrm{sw}}$, the existence of some macrodomain walls in the ''splitting relation'' with $\mathbf{H}_x$ is sufficient to complete the magnetization reversal. Note also that $H_{\mathrm{sw}}\propto d^{-1}$ and quickly falls off with increasing d. Both H_{sp} and H_{sw} are *intrinsic* properties for a given d, i.e., they exist even if there are no defects (antiphase boundaries) in the c-domains.

H_{sp} may be easily estimated micromagnetically for a (001) macrodomain wall. When its two partial macrodomain walls are displaced at distance L, the alternating magnetic charges appearing at the twin boundaries form a regular stack of ''capacitors'' (see Fig. 2). For $L\gtrsim d$, the magnetic field is concentrated inside these capacitors, and the total magnetostatic energy is proportional to L; the coefficient in this proportionality determines H_{sp}. Such a calculation gives $H_{\mathrm{sp}}=\pi M$ (or, alternatively, $H_{\mathrm{sp}}=H_a\eta/4$). The splitting threshold for (110) macrodomain wall is larger because of the magnetic charges on its segments. In the above estimate we neglected the deviation of $\mathbf{M}$ from the easy axis at distances $\sim\delta$ from the twin boundaries, which reduces H_{sp} for small d.

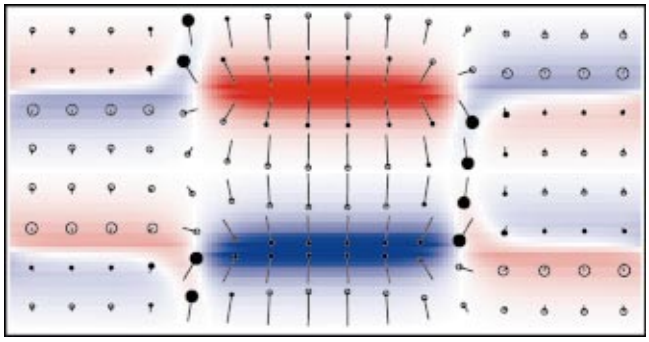

FIG. 2. (Color) Split (001) macrodomain wall in a stack with $d=32a_{\mathrm{bct}}$. Presentation is similar to Fig. 1(d).

Thus, at $\eta\ll1$ we have $H_{\mathrm{sp}}\ll H_a$. In particular, using the room-temperature values of M,[2] we obtain H_{sp} of 2.5 kOe for CoPt and 3.5 kOe for FePt and FePd. These values are close to the typical fields at which hysteresis is observed in these magnets. Quite naturally, they are much less than the coercive fields corresponding to uniform rotation of magnetization in the c-domains.[2] A peculiar feature of a partial macrodomain wall in the polytwinned crystal is that it separates qualitatively different magnetic domains with different free energies, and hence there is an intrinsic force acting on an isolated partial macrodomain wall (its density per unit cross section of the c-domain is $f_s=2MH_{\mathrm{sp}}$).

V. DOMAIN WALL SEGMENTS, PINNING, AND COERCIVITY

Real polytwinned alloys, as we noted above, usually contain a high density of antiphase boundaries in the c-domains. It is known that domain walls may be pinned by antiphase boundaries,[10] and it was argued that this mechanism may explain the high coercivity of CoPt type alloys.[7,8] Here we show that this pinning is indeed quite strong, but the ''dissociation'' of macrodomain walls into segments also has a profound effect on magnetization reversal.

The pattern of antiphase boundaries within c-domains determines the statistical properties of the random value $U(x)$ where x is the coordinate of a domain wall segment and U is its excess free energy induced by antiphase boundaries. For the following basic consideration we assume that $U(x)$ describes a distribution of similar pinning centers with the typical distance l_d between them. The maximal slope of $U(x)$ determines the *unpinning threshold* H_u, i.e., the value of the

field $\mathbf{H}_0 \| c$ required to unpin a single *c*-segment. Thus, in the absence of magnetostatic forces at $H_0 < H_u$ each *c*-segment is pinned, and at $H_0 > H_u$ it can move freely to the surface of the polytwinned stack. These assumptions are obvious for patterns with isolated antiphase boundaries as in Fig. 5 of Ref. 3 where $l_d \sim (5-10)d$; however, the main features of more complex patterns[4–6,8] may also be described by some characteristic values of H_u and $l_d \lesssim d$.

The maximum possible H_u is achieved when domain wall segments are parallel to isolated plain antiphase boundaries. To evaluate this maximum in the studied alloys, we explored[11] the modification of exchange and MCA at an isolated (101)-oriented antiphase boundary in CoPt, FePt, and FePd using the tight-binding linear muffin-tin orbital method. We found that the MCA is strongly suppressed at the antiphase boundary, leading to a domain wall *attraction* to the antiphase boundary with H_u of about 11, 7, and 1.5 kOe for CoPt, FePt, and FePd, respectively. These values significantly exceed the observed coercivities.[8] Since a high MCA is associated with $L1_0$ ordering, it is natural that local disorder at an antiphase boundary suppresses MCA.

Let us now explore the role of intrinsic magnetostatic forces in magnetization reversal. We restrict ourselves to the case of $\mathbf{H}_0 \| Ox$ in a single crystal with different types of polytwinned stacks (''single crystal'' refers to the parent fcc lattice). Such a field does not affect YZ-stacks, except for a reversible transverse magnetization. In other stacks $\mathbf{H}_0$ exerts a force density $f = 2MH_0$ on X-segments *only*.

From our definition of H_{sp} it follows that if *c*-PMDW in an X*c*-stack (c=Y or Z) is held in place (e.g., by pinning), then the free (unpinned) X-PMDW moves to infinity at $H_x \geqslant H_{sp}$ (neglecting the demagnetizing effects). At $H_x < H_{sp}$ the X-PMDW moves to a finite distance $L(H_x)$ from the *c*-PMDW. By definition, $L(H_{sp}) = \infty$. Except for a close vicinity of H_{sp}, $L \lesssim d$.

The path of magnetization reversal differs qualitatively in two cases: (a) $H_{sp} > H_u$, and (b) $H_{sp} < H_u$. In case (a) the macrodomain wall can only move as a whole (intrinsic pressure f_s is strong enough to unpin a partial macrodomain wall), but domain wall segments may to some extent ''adapt'' to the local pinning potential. Let us define the characteristic displacement l_m ''allowed'' by magnetostatic forces as $l_m = L(H_u)$. Obviously, l_m increases with H_u, and $l_m \to \infty$ at $H_u \to H_{sp}$. If $l_m > l_d$, the effective unpinning field of the macrodomain wall is $H_U \sim 2H_u$ ($\mathbf{H}_0$ affects one half of the domain wall segments, while all segments can be effectively pinned). However, as l_m becomes smaller than l_d, H_U is quickly reduced, because only a fraction of domain wall segments can be pinned simultaneously (macrodomain wall is effectively ''rigid'' and can not make ''kinks'' comparable with l_d).

Now, in case (b) the macrodomain wall may split in two partial macrodomain walls at sufficiently large $\mathbf{H}_0$. The macrodomain wall is ''soft,'' and each domain wall segment can be effectively pinned. During the whole cycle of remagnetization pinned Y- and Z-PMDW's do not move at all, and hence the intrinsic (magnetostatic) force acting on a moving X-PMDW will change its sign every time that it crosses, e.g., an Y-PMDW (in an XY-stack). Thus, for an X-PMDW we have $H_U = H_u + H_{sp}$. Different magnetization reversal properties may, in principle, be observed if the sample was previously magnetized to saturation by $\mathbf{H}_0$ along, e.g., (111). In this case there are no Y- and Z-PMDW's, and in some stacks the switching threshold is $H_U = H_u - H_{sp}$. The hysteresis loop in this case may have a peculiar double-step feature with magnetization jumps at $H_0 = H_u \pm H_{sp}$. Such ''hysteresis memory'' effects provide a test of the $H_{sp} < H_u$ relation and may be used to design ''programmable'' magnets.

Thus, for an initially demagnetized sample with the given H_u the coercive force H_c first rises with H_{sp}, reaches its maximum $\sim 2H_u$ at $H_{sp} \approx H_u$, stays roughly constant in the range $\infty > l_m > l_d$, and finally falls off at $l_m < l_d$. The high coercivity of CoPt is probably due to the fact that this magnet with suitable processing is close to the optimal $H_{sp} \sim H_u$ condition. By contrast, in FePd H_{sp} is too large ($H_{sp}/H_u \approx 2.3$ even for maximal possible H_u), so that $l_m \ll d$; this conclusion agrees with the relatively small observed H_c/H_a ratio.

In our analysis we neglected the demagnetizing fields. Close to saturation they are comparable to H_{sp}, but they have little effect on H_c, because they are small when the total magnetization is close to zero.

In conclusion, we developed a workable technique for the description of multiscale magnetization reversal phenomena in hard magnets and applied it to CoPt-type alloys. We have shown that the coercivity of these materials has at least two sources originating at different length scales: strong pinning of macrodomain walls by antiphase boundaries and their splitting at twin boundaries. This domain wall splitting seems to be a generic effect that may also affect magnetization reversal in other groups of materials, including some nanostripes[12] and multilayers; it may also occur at grain boundaries of certain misorientations.

ACKNOWLEDGMENTS

The authors are grateful to V.G. Vaks for useful discussions. This work was carried out at Ames Laboratory, which is operated for the U.S. Department of Energy by Iowa State University under Contract No. W-7405-82. This work was supported by the Director for Energy Research, Office of Basic Energy Sciences of the U.S. Department of Energy.

[1] R. Fischer and H. Kronmüller, Phys. Rev. B **54**, 7284 (1996); J. Fidler and T. Schrefl, J. Phys. D **33**, R135 (2000).

[2] N.I. Vlasova, G.S. Kandaurova, and N.N. Shchegoleva, J. Magn. Magn. Mater. **222**, 138 (2000).

[3] C. Leroux, A. Loiseau, D. Broddin, and G. van Tendeloo, Philos. Mag. B **64**, 58 (1991).

[4] C. Yanar, J.M.K. Wiezorek, and W.A. Soffa, in *Phase Transformations and Evolution in Materials*, edited by P. Turchi and A.

Gonis (TMS, Warrendale, 2000), p. 39.
[5] L.-Q. Chen, Y. Wang, and A.G. Khachaturyan, Philos. Mag. Lett. **65**, 15 (1992).
[6] K.D. Belashchenko, I.R. Pankratov, G.D. Samolyuk, and V.G. Vaks, J. Phys.: Condens. Matter **14**, 565 (2002).
[7] Ya.S. Shur *et al.*, Phys. Met. Metallogr. **26**, 241 (1968).
[8] B. Zhang and W.A. Soffa, Phys. Status Solidi A **131**, 707 (1992); Scr. Metall. Mater. **30**, 683 (1994).
[9] A. Aharoni, *Introduction to the Theory of Ferromagnetism* (Clarendon, Oxford, 1996).
[10] H. Kronmüller, J. Magn. Magn. Mater. **7**, 341 (1978).
[11] K.D. Belashchenko and V.P. Antropov, J. Magn. Magn. Mater. (to be published).
[12] M. Pratzer *et al.*, Phys. Rev. Lett. **87**, 127201 (2001).